

**A Relaxed Discrimination of 2'-O-Methyl GTP Relative to GTP Between *de novo* and Elongative RNA Synthesis by the Hepatitis C RNA-Dependent RNA Polymerase NS5B**

Hélène Dutartre, Joëlle Boretto, Jean Claude Guillemot, and Bruno Canard

*From the Centre National de la Recherche Scientifique and Universités d'Aix-Marseille I et II, UMR 6098, Architecture et Fonction des Macromolécules Biologiques, Ecole Supérieure d'Ingénieurs de Luminy-Case 925, 163 avenue de Luminy, 13288 Marseille cedex 9, France.*

Corresponding Author: Bruno Canard

Tel: +33-491 82 86 44

Fax: +33-491 82 86 46

Email: [bruno@afmb.cnrs-mrs.fr](mailto:bruno@afmb.cnrs-mrs.fr)

Running Title: Change of NTP selectivity by HCV NS5B during RNA synthesis

## SUMMARY

Several nucleotide analogues have been described as inhibitors of NS5B, the essential viral RNA dependent RNA polymerase of the Hepatitis C virus. However, their precise mode of action remains poorly defined at the molecular level, much like the different steps of *de novo* initiation of viral RNA synthesis. Here, we show that before elongation, *de novo* RNA synthesis is made of at least two distinct kinetic phases, the creation of the first phosphodiester bond being the most efficient nucleotide incorporation event. We have studied 2'-O-methyl GTP as an inhibitor of NS5B-directed RNA synthesis. As a nucleotide competitor of GTP in RNA synthesis, 2'-O-methyl GTP is able to act as a chain terminator and inhibit RNA synthesis. Relative to GTP, we find that this analogue is strongly discriminated against at the initiation step (~150-fold) compared to ~2-fold at the elongation step. Interestingly, discrimination of the 2'-O-methyl GTP at initiation is suppressed in a variant NS5B deleted in a subdomain critical for initiation (the "flap", encompassing aa 443 to 454), but not in P495L NS5B which shows a selective alteration of transition from initiation to elongation. Our results demonstrate that the conformational change occurring between initiation and elongation is dependent on the allosteric GTP-binding site, and relaxes nucleotide selectivity. RNA elongation may represent the most probable target of 2'-modified nucleotide analogues as it is more permissive to inhibition than initiation.

## INTRODUCTION

The Flaviviridae is an important virus family comprising three genera, namely flavivirus, pestivirus, and hepacivirus. Both flavivirus and hepacivirus genera comprise major human pathogens, such as Dengue virus, West Nile virus, Yellow Fever virus, and the Hepatitis C virus (HCV), respectively. The discovery of HCV in the late 1980's and analysis of its prevalence in the general population has revealed that HCV is the most common ethiological agent of chronic liver disease (1). More than 170 millions persons are infected by HCV in the world, making these individuals at risk to develop liver cirrhosis and hepatocellular carcinoma (2). Unlike other viral diseases for which antiviral therapies exist (e.g., Human Immunodeficiency virus or Herpes infections), a persistent HCV infection can be controlled (3,4). In some cases, HCV can be eradicated from an infected patient (5), and this represents the first example of a complete success of antiviral therapy ever.

Current antiviral therapies rely on the association of interferon  $\alpha$  to the nucleoside analogue Ribavirin. Ribavirin is a broad spectrum antiviral agent discovered about 30 years ago. Although not effective on all HCV isolates and associated with undesirable side effects (6), Ribavirin exerts its antiviral activity by at least two mechanisms which are intimately linked. First, it is intracellularly converted to Ribavirin 5'-monophosphate which is a potent inhibitor of the cellular inosine 5'-monophosphate dehydrogenase (IMPDH) (7,8). Inhibition of IMPDH depresses the intracellular concentration of GTP. Second, Ribavirin is also converted to RTP and acts as a GTP analogue. It is incorporated into viral RNA, leading to lethal mutagenesis of the viral genome (9), and also inhibits the polymerase directly after its incorporation (9-11). Thus, IMPDH inhibition and subsequent depression of cellular GTP pools potentiates the action of RTP as an antiviral nucleotide analogue.

The antiviral action of Ribavirin as a nucleotide analogue indicates not only that the HCV polymerase is an interesting target for antiviral drugs but also that nucleosides in general are interesting molecules to develop potent anti-HCV treatments. Therefore, several nucleoside analogues are currently being evaluated as potential anti-HCV agents, such as 2'-O-methyl nucleosides, 2'-C-methyl nucleosides, and  $\beta$ -D-N<sup>4</sup>-hydroxycytidine (12-14), or canonical 3'-deoxyribonucleotides (15).

A clear picture of the mechanism of action of some of these inhibitors is beginning to emerge. In the case of  $\beta$ -D-N<sup>4</sup>-hydroxycytidine, no direct inhibition of the polymerase is observed using the purified enzyme in *in vitro* assays (12). Rather, it is thought that the analogue 5'-monophosphate is incorporated into the viral RNA selectively leading to biologically inactive genomes. In the case of 2'-modified analogues, it has been reported that they act as non-obligate chain terminator of RNA synthesis (14). Unlike obligate chain terminators (e.g., AZT, 2'3'-dideoxynucleosides in antiretroviral treatments), non-obligate chain terminators carry a 3'-hydroxyl group, and thus bear potential to support further RNA synthesis once incorporated into viral RNA.

Most of our understanding of the mechanism of action of nucleoside analogues comes from studies performed on the HIV-1 reverse transcriptase (RT) and its nucleoside inhibitors (for recent reviews, see (16,17)). RT is a DNA and RNA primer-dependent DNA polymerase. The HCV polymerase, however, is an RNA polymerase able to initiate RNA synthesis without primer in a so called *de novo* RNA synthesis process, as well as to elongate an existing RNA primer (18-20). Primer independent RNA synthesis is unique to viral RNA polymerases so far. To perform such an initiation step, these polymerases have selected through evolution unique structural features essential to the synthesis of their own short RNA primers (21-23). The crystal structure of the HCV polymerase as well as some elegant enzymatic assays have identified such a structure (23-25). A  $\beta$ -strand-turn- $\beta$ -strand ("flap")

subdomain is actually obstructing the polymerase active site when the latter is compared to related primer-dependent polymerases. Based on both structural and deletion studies, it has been proposed that the flap is giving physical support to initiating nucleotides, up to the point where the neo-synthesized primer RNA triggers a conformational change of the polymerase active-site (23,24,26). Subsequently, the polymerase has to adopt an alternate conformation in which the primer is elongated in a processive fashion. Recently, the flap has been shown to play a role in repressing primer-directed RNA synthesis in favor of initiation of RNA synthesis (27). The HCV polymerase has been reported to be activated by GTP, which is able to bind to a low affinity allosteric site away from the polymerase active site (23). It is suspected that the action of GTP at this allosteric site plays a role in the triggering of the switch between initiation and elongation. These distinct steps of RNA synthesis are not clearly characterized, either structurally or kinetically.

This context of poorly defined mechanisms of RNA synthesis impedes precise evaluation of the inhibition potency of nucleotide analogues. 2'-modified analogues are not obligate chain-terminators. Therefore, a viral RNA terminated with such an analogue is expected to abort viral synthesis, hence the observed antiviral effect, but a 2'-modified nucleoside monophosphate incorporated into viral RNA and further elongated is also expected to exert an antiviral effect through the production of structurally altered progeny RNA genomes. Not known with precision either are the extent of discrimination of these analogues at the HCV polymerase active site during the initiation or elongation step.

Clearly, a better understanding of the different steps of RNA synthesis is needed, as well as a molecular basis for the evaluation of inhibitor potency. This should aid the design of potent HCV inhibitors and the *in vivo-in vitro* correlation of their antiviral effect, as well as the anticipation of future potential resistance mechanisms that might develop upon sustained treatments.

In this paper, we contribute to the characterization of the initiation step of RNA synthesis. We have made use of 2'-O-methyl GTP to dissect the effect of this GTP analogue on NS5B at the level of allosteric activation, inhibition of initiation and elongation of RNA. We report discrimination values of this analogue relative to GTP during the initiation and elongation phases of RNA synthesis. We show that there is a marked discrimination of this analogue at the initiation of RNA synthesis, but not when RNA synthesis reaches the elongation phase.

## RESULTS

GTP plays a special role during viral RNA synthesis by HCV NS5B. It is the initiating nucleotide of (+)RNA genome synthesis, it is incorporated throughout the genome during the elongation process, and its concentration is perhaps regulating these steps through binding to an allosteric site (23,28,29). Therefore, the mode of action of GTP analogues (such as RTP) is expected to be complex. We have made use of a known GTP analogue inhibitor, 2'-O-methyl GTP to dissect kinetically the different mechanisms at work during initiation and elongation of RNA synthesis.

*The Target of 2'-O-methyl GTP and its Inhibition Kinetics* – When polyC is used as a template of RNA synthesis, the appearance of polyG RNA products is biphasic (Fig. 1A). The initial rate of RNA synthesis can be measured during the linear phase of the reaction, and the addition of increasing concentrations of 2'-O-methyl GTP to the reaction decreases this rate of synthesis. The decrease of synthesis rate, i.e. inhibition, can be plotted as a function of 2'-O-methyl GTP synthesis, giving a 50 % inhibitory concentration ( $IC_{50}$ ) of  $3.5 \pm 0.2 \mu\text{M}$  (Fig. 1B). In an attempt to characterize further the mechanism of 2'-O-methyl GTP inhibition, a traditional Henri-Michaelis-Menten analysis was performed, and the reciprocal Lineweaver-Burke plot is shown in Fig. 1C. The 2'-O-methyl GTP analogue exhibits some features of a competitive inhibitor. However, above  $200 \mu\text{M}$  of GTP, all experimental curves merge with the uninhibited ( $I = 0$ ) reaction curve, indicating that 2'-O-methyl GTP ceases to exert its inhibitory activity. This non-linear behavior indicates that several phenomena are taking place in the same enzyme site and/or time, and thus, the kinetics of initiation and elongation of RNA were studied for between the GTP and its competing analogue.

*Kinetics of the Initiation Phase of RNA Synthesis Using GTP* - The initiation phase of RNA synthesis is defined as the formation of the first phosphodiester bond between two

nucleotides to form a ribo-dinucleotide primer. In the case of the HCV polymerase, structural studies have indicated that the active site is closed by the flap on one side and the fingers on the other side (Fig. 2). Thus, one can envision that nucleotides are polymerized up to a certain extent into RNA primers, then the active site has to open up to adopt a processive mode of elongative synthesis. These steps can be illustrated by a polymerization reaction analyzed with a gel assay. In this assay, an oligonucleotide of 15 consecutive cytidines (oligo(C)<sub>15</sub>) is used as a template to direct RNA synthesis using GTP as the sole nucleotide substrate. Fig. 3A shows a kinetic order of appearance of oligoG products. The size distribution of products generated using the oligoC<sub>15</sub> template is identical to that obtained using polyC (not shown). Abortive 6-mers products or less are accumulating over time, whereas products > 6-mers are rapidly and processively converted to 15-mers (template-length, or G<sub>15</sub>) final products. In fact, a closer examination of the reaction products reveals that the overall reaction can be kinetically split into three phases (Fig. 3B). First, the very first phosphodiester bond formation from G<sub>1</sub> to G<sub>2</sub> occurs rapidly and G<sub>2</sub> products accumulate over time. Second, abortive products up to G<sub>6</sub> are formed. Subsequently, a third phase occurs in which G<sub>6</sub> products are elongated processively into full-length, run-off products. Fig. 3C shows the individual quantitation of reaction products. A band-product accumulating over time indicates a rate-limiting step for the subsequent phosphodiester bond formation. It is apparent that, out of the final G<sub>15</sub> product, G<sub>2</sub> and G<sub>5</sub> are accumulating more than G<sub>3</sub>, G<sub>4</sub>, and G<sub>6</sub>. Very similar patterns of product formation are observed in the presence of higher GTP concentrations (see "Supplementary Material", Fig. 3 bis.), as well as for a variety of templates (not shown). We conclude that, as opposed to the commonly reported hypothesis (30,31), the true initiation reaction of formation of the G<sub>2</sub> product is not rate-limiting, even at low GTP concentrations of 10  $\mu$ M such as those used here. Instead, it is the next reaction from G<sub>2</sub> to G<sub>3</sub> which is rate-limiting together with another slow rate reaction from G<sub>6</sub> to highly polymerized products. The

formation of  $G_2$ , of  $G_3$  to  $G_6$ , and of  $>G_6$  products will be referred to as the initiation, transition, and elongation reaction, respectively. The initiation reaction was examined in greater kinetic details for GTP and 2'-O-methyl-GTP comparatively.

*Kinetic Analysis of the  $P_1$  to  $P_2$  Reaction, and its Inhibition by 2'-O-methyl-GTP* – The kinetics of  $P_2$  product formation was examined using a gel assay as described above (Fig. 4A). In order to examine a single nucleotide incorporation and simplify the analysis, we made use of a short oligonucleotide template allowing the extension of a single GTP or 2'-O-methyl GTP. As reported by others for such a template (32), the HCV polymerase is able to initiate RNA synthesis at two sites, giving rise to the desired product pppGC and an unavoidable pppCC by-product with no incidence in the calculations since the CTP concentration was kept constant throughout all the experiments. First of all, 2'-O-methyl GTP is not a chain terminator since pppGmC is formed in a 2'-O-methyl GTP concentration-dependent manner. This pppGmC product is further elongated into pppGmCC in a 2'-O-methyl GTP concentration-dependent manner, albeit very inefficiently (see Fig. 4). However, whether or not this low level  $P_3$  formation is taken into account in the calculation does not change significantly the kinetic constant values of the  $P_1$  to  $P_2$  reaction.

Such experiments allowed to determine an apparent Henri-Michaelis-Menten constant  $K_M$  and a maximum velocity  $V_{max}$  for GTP and 2'-O-methyl GTP (Fig. 4B). For a given nucleotide, the ratio  $V_{max}/K_M$  represents the efficiency of  $P_2$  formation under steady-state conditions, and allows the determination of nucleotide selectivity at the polymerase active site. The values are reported in Table I. The presence of the 2'-O-methyl group has a major effect on the kinetics of the reaction, as judged by a  $> 20$ -fold increase in  $K_M$  and a  $> 6$ -fold decrease in the maximum velocity  $V_{max}$  (Table I, WT columns). Comparison of the resulting efficiencies of incorporation gives a 148-fold selectivity, i.e., preference for GTP relative to 2'-O-methyl GTP at this step of the reaction. Further work is needed to determine if, under

these conditions,  $K_M$  faithfully reflects the dissociation constant  $K_D$  of GTP from the RNA:polymerase complex or from the free polymerase before template binding. However, the presence of methyl group in 2' of the initiating nucleotide produces a much larger effect on  $K_M$  than on  $V_{max}$ , so we can safely conclude that 2'-O-methyl GTP is essentially discriminated through an altered binding affinity at the initiation nucleotide binding site of the HCV polymerase.

*Comparative Inhibition Kinetics of the Initiation and Elongation Reactions* – The effects of 2'-O-methyl GTP were next examined in the context of initiation followed by elongation of neo-synthesized RNA. We used an oligoC<sub>15</sub> template allowing multiple incorporations of either GMP or the inhibitor 2'-O-methyl GMP into RNA, and the products were analyzed using a gel assay as described above. An additional radiolabeled product appears upon gradual increase of 2'-O-methyl GTP in the reaction (Fig. 5A). This product was identified as GMP upon its co-migration with a GMP control under several electrophoresis conditions as well as upon HPLC analysis (not shown). At a saturating GTP concentration of 100  $\mu$ M ( $K_{M(GTP)} = 8.5 \mu$ M, Table I, WT columns) and a 2'-O-methyl GTP concentration of 200  $\mu$ M (i.e., around the  $K_{M(2'-O-methyl\ GTP)}$ , Table I, WT columns), the synthesis of this futile GMP product accounts for ~28 % of the total products of the reaction ( $K_{M(GMP)} = 60 \mu$ M,  $V_{max} = 0.1 \cdot 10^{-3} \text{ sec}^{-1}$ ). We do not observe an accumulation of GMP when the polymerization reaction is performed with  $\alpha$ -<sup>32</sup>P GTP as the sole nucleotide, even if the GTP concentration is increased to 200  $\mu$ M (see "Supplementary Material", Fig. 3 bis) or to 800  $\mu$ M (not shown), although we can clearly observe an accumulation of GMP with 100  $\mu$ M of 2'-O-methyl GTP (figure 5A). Moreover, no CMP accumulation is observed when  $\alpha$ -<sup>32</sup>P-CTP is used instead of  $\alpha$ -<sup>32</sup>P GTP (Fig. 4), ruling out the presence of a contaminating phosphatase in the assays. A probable interpretation of the appearance of GMP is that 2'-O-methyl GTP occupies the initiation nucleotide binding site  $N_1$ , and the presence of the 2'-O-methyl group impedes proper

positioning of GTP at the N<sub>2</sub> site. Yet the α-phosphate of GTP would be activated to receive a nucleophilic attack coming from a water molecule instead of the initiating nucleotide 3'-OH. The size distribution of polymerization products was determined as a function of 2'-O-methyl GTP concentration under the linear phase of product formation. The results are presented in Fig. 5B. Again, the G<sub>2</sub> to G<sub>4</sub> products accumulated over time, reaching a concentration almost independent from the concentration of 2'-O-methyl GTP, whereas products > G<sub>4</sub> in size decreased sharply upon increasing concentration of the inhibitor. This demonstrated that 2'-O-methyl has a much greater effect on elongation synthesis than on the initiation and transition reactions. The discrimination of 2'-O-methyl GTP at the elongation phase of RNA synthesis was thus investigated further.

*Kinetics of the Elongation Reaction Inhibition by 2'-O-methyl GTP* – We made use of a hairpin RNA primer template and gel assay to study the effect of 2'-O-methyl GTP on the elongation reaction (Fig. 6A). Such a primer/template system has been described to mimic the elongation reaction (13,14). Indeed, the seven base-paired double stranded RNA and its loop is unable to be accommodated in the initiation site, and the nucleotide used does not allow *de novo* initiation of RNA synthesis. The results are presented in Table II. Under these conditions, GTP is bound with a 5-fold lower apparent affinity ( $K_{M(GTP)} = 47 \mu\text{M}$ ) than at the initiation step ( $K_{M(GTP)} = 8.5 \mu\text{M}$ , Table II, WT columns). It is noteworthy that the initiation reaction P<sub>1</sub> to P<sub>2</sub> is in fact more efficient than the elongation reaction, in agreement with the qualitative results presented in Fig.3, and the resulting proposition that initiation is not rate-limiting. A change in K<sub>M</sub> between initiation and elongation has been described by others (19,29), but with an opposite trend showing a less efficient initiation than elongation (see discussion). It may well be, however, that subsequent incorporations and the conformational change required to enter the elongation phase represent the true rate-limiting step. The 2'-O-methyl analogue was found to be a much better substrate during elongation than during the

initiation reaction, with a  $K_{M(2'-O\text{-methyl GTP})}$  value of 36  $\mu\text{M}$ . Remarkably, the overall discrimination of the 2'-O-methyl analogue was reduced to a value of  $\sim 2$ , mainly because the natural substrate GTP becomes a 5-fold less efficient substrate. We conclude that there is a marked relaxation of 2'-O-methyl group discrimination at the polymerase active site between the initiation and elongation steps, leading to a 70-fold increase of the sensitivity to the inhibitor after the enzyme has entered the elongation phase.

*Structural Determinants of Nucleotide Selectivity at the Initiation Step* – The initiation step is thought to involve a small  $\beta$ -sheet structure, the flap, to position the initiating nucleotide precisely (23,24,27). Once initiation has taken place, the flap has to move away in order to let the nascent dsRNA going out of the active site. It has been speculated that a GTP molecule bound at the allosteric active site can trigger/modulate the required conformational change between initiation and elongation (23,28). Therefore, both the flap and the allosteric active site are somehow connected to this conformational change, and thus to the transition from initiation to elongation. Deletion of the flap ( $\Delta$ -flap) renders an active HCV RNA polymerase (Fig. 6B and (24)). Likewise, Proline 495 is in the allosteric GTP binding site, and the P495L substitution diminishes GTP binding while retaining an active HCV polymerase (28). The  $\Delta$ -flap and P495L polymerases were generated and studied for 2'-O-methyl GTP discrimination at initiation (Table I) and elongation (Fig. 6B and Table II, commented in the next section below).

Surprisingly, deletion of the flap has only a modest effect on GTP incorporation kinetics during the initiation reaction (Table I). The GTP incorporation efficiency drops an overall 4-fold as judged by corresponding  $V_{\text{max}}/K_M$  values. However, 2'-O-methyl GTP becomes an actual 2.3-fold better substrate upon deletion of the flap, giving rise to a 17-fold discrimination relative to GTP. Compared with the 148-fold discrimination of the wild-type enzyme, this 17-fold discrimination corresponds to a  $> 8$ -fold relaxation of analogue

selectivity upon deletion of the flap. The P495L substitution has no effect, with an overall discrimination of 157-fold compared to the 148-fold measured for the wild-type enzyme. We conclude that the flap is critical in the stringency of assembly of the initiation complex, whereas the allosteric site has no effect at this stage.

*Structural Determinants of Nucleotide Selectivity at the Elongation Step* – Both the  $\Delta$ -flap and P495L polymerases were also studied comparatively to the wild-type enzyme during the elongation phase of RNA synthesis. The P495L mutation renders an enzyme of too low elongation activity to measure steady-state parameters accurately, indicating that either the transition or/and elongation are affected by this point mutation. To investigate further which of the latter two steps is altered by the P495L substitution, a gel assay was used, and the results are presented in Fig. 7A. As expected, the synthesis of  $G_2$  products is barely affected by the presence of P495L, whereas a clear decrease in abundance of products greater in size than  $G_4$  is observed. Plotting the comparative abundance of products is shown in Fig. 7B. The relative decrease in abundance of products greater in size than  $G_4$  is striking in the case of P495L relative to the wild-type enzyme. We conclude that P495L alters the switch from transition to elongation specifically. Since the proline 495 residue is involved in binding GTP at the allosteric site and that the P495L substitution abrogates GTP-binding (23,27,28), we conclude that a GTP molecule must be bound at this site to allow the transition/elongation switch, after which NS5B becomes much more permissive to 2'-O-methyl GTP inhibition.

Has the flap any role in nucleotide selection during elongation? Discrimination of 2'-O-methyl GTP was measured during the elongation phase using the hairpin template/primer system and the  $\Delta$ -flap polymerase (Fig 6B). The results are reported in Table II. Deletion of the flap yields an RNA polymerase which incorporates GMP into RNA 550-fold more efficiently than the wild-type enzyme (compare  $V_{max}/K_M$  in Table II, and panel A and B in Fig. 6B), the increase in efficiency coming more from an increased  $V_{max}$  than from a decreased  $K_M$ .

A similar trend is observed using 2'-O-methyl GTP, as deletion of the flap yields a 232-fold improvement of the overall incorporation efficiency of this analogue. Unlike during initiation where discrimination is relaxed upon deletion of the flap, discrimination of the 2'-O-methyl group is modestly increased (from 2.3- to 5.5-fold) during elongation.

Taken together, these results indicate that the flap has a major role in the precise assembly of the initiation complex, as reflected by a high nucleotide analogue discrimination. The allosteric GTP-binding site is critical for an efficient switch from transition to elongation. Once re-arranged into the elongation mode, the flap does not seem to play a significant role in nucleotide selection, as reflected by an increased permissivity towards the presence of a 2'-O-methyl group in the incoming nucleotide.

## **DISCUSSION**

The viral RNA-dependent RNA polymerase NS5B plays an essential role in the replication of the HCV RNA genome. NS5B has no homologue in the human cell, and is a validated target for antiviral drug-design (33,34). During RNA replication, NS5B performs highly specialized tasks such as *de novo* initiation of RNA synthesis and elongation of the nascent genomic or antigenomic RNA strand. Using the HIV-RT crystal structure as a model (35), structural work on NS5B has shown that the transition from initiation to elongation must occur with a concomitant conformational change, involving mainly the flap which would otherwise obstruct the active site during elongation. Are there any mechanistic constraints associated with this conformational change? Is there any variation in the potency of inhibition by nucleotide analogues during the different phases of RNA synthesis? In addressing these questions, our study contributes to the mechanistic characterization of *de novo* RNA synthesis, RNA elongation, and the switch between these two steps.

The *de novo* initiation of RNA synthesis is commonly referred to as primer-independent RNA synthesis steps before processive, primer-dependent RNA synthesis (18-20,26,29,31,36-38). In the present work, we characterize *de novo* initiation kinetically, and propose to break down *de novo* initiation into several phases. The first one is the creation of the first dinucleotide. As shown here (Figs 3, 4, 5, 7 and Table I), it is a very efficient reaction compared to subsequent polymerization events. We call this step initiation, and transition the following steps occurring before the enzyme adopts a processive, elongative RNA synthesis mode. This proposition is based on the unexpected kinetic properties of diribonucleotide synthesis. Contrary to common beliefs (30,31), we found that initiation is not rate-limiting. Instead, we have identified that the P<sub>2</sub> to P<sub>3</sub> reaction constitutes the main rate-limiting step. The next phase is a transition phase where products from P<sub>3</sub> to P<sub>5</sub> are synthesized in a distributive manner, with another slow rate reaction from P<sub>5</sub> to highly polymerized products. At this stage, there is a clear involvement of the allosteric GTP binding site to allow processive synthesis (Fig. 7) to take place. It is tempting to speculate that this second rate limiting step corresponds to an opening of the flap allowing a fast, processive RNA synthesis corresponding to the elongation phase. It is interesting to note that this enzyme behavior is sequence-independent (unpublished data) as it has been also observed in a very recent study (39), where abortive P<sub>2</sub> to P<sub>6</sub> products are generated in addition of the full-length RNA product. In other words, no matter which nucleotides are polymerized, the P<sub>2</sub> to P<sub>3</sub> reaction constitutes the rate-limiting step together with another slow rate reaction from P<sub>5</sub> to larger products. We interpret this finding as a reflection of active site constraints. Whether a conformational change occurs from P<sub>2</sub> to P<sub>3</sub> is an interesting question as unlike elongation, *de novo* RNA synthesis has been shown to be more dependent on Mn<sup>2+</sup> than on Mg<sup>2+</sup> (29,32). A high GTP concentration has been reported to be needed to promote efficient *de novo* synthesis (38,40). In light of the present work and recent work (27,39), such high GTP concentration is

more likely required to avoid primer-dependent RNA synthesis, and/or at the transition step to overcome the two rate limiting steps, and/or to trigger the conformational change dependent on the GTP-binding site. However, in experiments such as shown in Fig. 3, we never observed any specific  $P_2 - P_6$  band product disappearing faster than others upon increasing the GTP concentration (see Fig. 3 bis in "Supplementary Material"). This favors the proposition that the role of the high GTP concentration is to repress primer-dependent synthesis rather than accelerate either the catalytic step or a conformational change.

A 2'-O-methyl GTP molecule is able to interfere significantly with one of the three RNA synthesis steps, namely elongation. Our data is in agreement with Carroll *et al.* (14) who showed that the related analogue 2'-O-methyl CTP acts as a chain terminator, but without quantitating the extent of discrimination relative to its natural counterpart CTP. Out of the scope and not reported in our present work is the observation that, indeed, there is almost no chain extension of a 2'-O-methyl GMP terminated RNA chain (14). Our data show that this analogue is highly discriminated against during initiation (~150-fold) and transition, whereas it is almost equally incorporated as GTP during elongation. It could be argued that once 2'-O-methyl GTP is positioned as the initiating nucleotide ( $N_1$  position), the high discrimination we observe is a mere result of its inability to be extended. However,  $K_M$  increases 24-fold from 8.5 to 205  $\mu\text{M}$  upon the presence of the 2'-O-methyl group, making likely that impaired binding of the analogue is truly responsible for resistance at initiation. Very precise and tight molecular interactions of these initiation complexes may be required for proper alignment of the catalytic centers of nucleotide substrates. This may translate into a highly stringent nucleotide selection and hence, an increase in discrimination and natural drug-resistance at initiation. During elongation, the nascent nucleic acid has to move almost freely in the polymerase active site, and the polymerase must then adopt a more flexible conformation, reflected by a relaxed nucleotide selectivity.

A more stringent, selective initiation complex is illustrated by our experiments making use of the  $\Delta$ -flap enzyme. Deletion of the flap has at least three consequences. It renders an enzyme slightly altered for the creation of the first phosphodiester bond (~4-fold, Table I), with relaxed selectivity against 2'-O-methyl GTP (~8-fold, Table I), and much more active for elongation (~550-fold, Table II). It would be interesting to perform these experiments in the context of an authentic 5'-genomic RNA:replicative complex (including a full-length NS5B polymerase). Our findings suggest that the flap plays a role in the stabilization of this initiation complex, in agreement with recent work (27), and that this stringency of initiation is made at the expense of the overall polymerization efficiency. Whether this finding holds true for other nucleotide analogues such as 2'-methyl or 3'-deoxy NTP remains to be determined. Drawing on the HIV-RT experience, precise knowledge of the inhibited step will endow considerable importance when several NS5B polymerase inhibitors are to be combined during therapeutic interventions. Indeed, different inhibitor types specify distinct resistance mechanisms, and mechanistic information is important to predict and understand cross-resistance, and optimize drug combinations.

## EXPERIMENTAL PROCEDURES

### *HCV 1b polymerase plasmid constructions, enzyme preparation, and reagents -*

Several reports (27,39) mention that the authentic C-terminal part of NS5B is critical in the repression of primer-dependent synthesis in favor of initiation. Since we did not examine both RNA synthesis modes simultaneously, all NS5B proteins were truncated at their C-terminus by 55 residues, and six histidine residues were added to the C-terminus of each of the proteins to facilitate affinity purification. The resulting NS5B is called wild-type NS5B throughout the manuscript, and it is unlikely that the former has a C-terminus extending long enough to reach the active site (Fig. 2), as described for a 21 amino acids C-terminus truncated NS5B (41,42). NS5B wild-type or mutant proteins were expressed from the pDest 14 vector (Invitrogen) in *E. coli* BL21(DE3) cells (Novagen). Site directed mutagenesis was made using the Quick Site-directed mutagenesis Kit according to the manufacturer's instruction (Stratagene). All constructions were verified by DNA sequencing. NS5B proteins were purified from bacteria grown at 37 °C in LB medium supplemented with ampicillin (100 µg/ml) and chloramphenicol (17 µg/ml) and induced with 50 µM IPTG during 16-18 hours at 17 °C. Bacteria were harvested by centrifugation, and recombinant RdRps were purified in sodium phosphate buffer through a Talon cobalt affinity column (Invitrogen) followed by SP-sepharose column chromatography (Amersham). Eluted proteins were concentrated to 2 mg/ml and stored at -20°C. No attempts were made to titrate the active site concentration of NS5B preparations. Therefore, maximum velocity values  $V_M$  related to total enzyme concentration are reported instead of  $k_{cat}$  values throughout the manuscript (see Tables). RNA molecular weight markers were synthesized using T7 RNA polymerase (T7 RNAP) and the appropriate template RNA. For this purpose, reactions were performed in T7 buffer (40 mM Tris HCl pH 7.5, 6 mM MgCl<sub>2</sub>, 2 mM spermidine, 10 mM DTT) at 30 °C for 10 min, using 10

ng of DNA oligonucleotide (5'-TTTTTTTTTTTTTTTTTTTTTTCCTATAGTGAGTCGTATTA-3' or 5'-TTTTTTTTTTTTTTTTTTTTTCCCCCTATAGTGAGTCGTATTA-3') template annealed to the T7 primer (5'-TAATACGACTCACTATAGGG-3'), and 10  $\mu$ M  $\alpha$ -<sup>32</sup>P-GTP (1  $\mu$ Ci). Reactions were initiated by the addition of 1 $\mu$ g of recombinant T7 RNAP. The GMP marker was synthesized through hydrolysis of  $\alpha$ -<sup>32</sup>P-GTP by Tobacco Acid Pyrophosphatase (Sigma) according to the manufacturer's instruction. RNA oligonucleotides were obtained from MWG-Biotech, homopolymeric cytosine template was obtained from Amersham-Pharmacia. DNA oligonucleotides were obtained from Lifetechnologies. For elongation experiments, RNA oligonucleotides were 5'  $\alpha$ -<sup>32</sup>P-labeled using T4 polynucleotide kinase (New England Biolabs).  $\gamma$ -<sup>32</sup>P-labeled adenosine 5'-triphosphate (3000 Ci/mmol),  $\alpha$ -<sup>32</sup>P-labeled guanosine 5'-triphosphate (3000 Ci/mmol),  $\alpha$ -<sup>32</sup>P-labeled cytosine 5'-triphosphate (3000 Ci/mmol), and uniformly labelled [<sup>3</sup>H]-GTP (5.20 Ci/mmol) were purchased from Amersham-Bioscience. 2'-O-methyl GTP was purchased from Trilink, Inc.

*Inhibitory concentration 50% (IC<sub>50</sub>) and Ki determination* - The 2'-O-methyl GTP concentration leading to 50% inhibition of NS5B-mediated RNA synthesis was determined in RdRp buffer containing 100 nM of homopolymeric cytosine RNA template, 0.1 mM [<sup>3</sup>H]-GTP (0.5  $\mu$ Ci), and 2'-O-methyl GTP (0, 0.1, 1, 2.5, 5, 7.5, 9, 10, 15, 20, 25  $\mu$ M). Reactions were initiated by the addition of 1 $\mu$ M of NS5B, incubated at 30°C, and stopped after 3 min by spotting aliquots onto DE-81 paper discs (Whatman International Ltd.). Filter paper discs were washed three times for 10 min in 0.3 M ammonium formate, pH 8.0, washed two times in ethanol, and dried. The radioactivity bound to the filter was determined using liquid scintillation counting. IC<sub>50</sub> was determined using the equation:

$$\% \text{ of active enzyme} = 100 / (1 + (I)^2 / IC_{50}) \quad (\text{Eq. 1})$$

where I is the concentration of inhibitor.  $IC_{50}$  was determined from curve-fitting using Kaleidagraph (Synergy Software).

*Steady state incorporation of nucleotide into homopolymeric templates* - Polymerase activity was assayed by monitoring the incorporation of radiolabeled guanosine on 15-mers cytosine RNA oligonucleotide template. All indicated concentrations are final. The reaction was performed in RdRp buffer (50 mM HEPES pH 8.0, 10 mM KCl, 5 mM  $MnCl_2$ , 5 mM  $MgCl_2$ , 10 mM DTT, 0.1 mg/ml BSA, 0.5 % Igepal CA630) containing 10  $\mu$ M or 100  $\mu$ M GTP as indicated, 1  $\mu$ Ci  $\alpha$ - $^{32}$ P-GTP, and 10  $\mu$ M RNA oligonucleotide. Reactions were initiated by the addition of 1  $\mu$ M purified NS5B and incubated at 30 °C. Aliquots were withdrawn over time from 10 s to 1 h. For inhibition analysis, increasing concentration of 2'-O-methyl GTP (10, 50, 100, 200 or 400  $\mu$ M) were added before the addition of NS5B, and reaction allowed to proceed for 30 min. Reaction products were separated using sequencing gel electrophoresis (20% acrylamide, 7 M Urea in TTE buffer (89 mM Tris, 28 mM Taurine, 0,5 mM EDTA)), and quantitated using photo-stimulated plates and a FujiImager (Fuji).

The formation of products was fitted with a burst equation:

$$(P) = A.(1-\exp(-(V_i.t)) + k_{ss}.t) \quad (\text{Eq. 2})$$

where A is the amplitude of the burst,  $V_i$  is the initial velocity of the reaction, and  $k_{ss}$  is the enzyme turn over rate.

*Determination of  $V_{max}$  and  $K_M$*  - An RNA oligonucleotide corresponding to the 3' end of the negative strand of the HCV genome (RNA H (-) 5'-UCGGGGGCUGGC-3') was used to analyze the synthesis of the first phosphodiester bond. The RNA H (-) template (10  $\mu$ M) was mixed in RdRp buffer with 1 $\mu$ M of NS5B. The reactions were started by addition of 100  $\mu$ M  $\alpha$ - $^{32}$ P-CTP (1  $\mu$ Ci), GTP (1, 5, 10, 50, 100, 500  $\mu$ M), and incubated at 30°C. Elongation was measured with a 5'  $\alpha$ - $^{32}$ P-labeled hairpin-RNA template (5'-UGACGGCCCGG AAAACCGGGCC-3'). The hairpin-RNA template (1 $\mu$ M) was mixed with 1  $\mu$ M of NS5B in

RdRp buffer before the addition of GTP (1, 5, 10, 50, 100, or 500  $\mu\text{M}$ ), and reactions were incubated at 30°C for 1 to 30 min. Initiation or elongation reactions involving 2'-O-methyl GTP were conducted using 2  $\mu\text{M}$  of enzyme to allow accurate measurement of low incorporation rates. All maximal velocities  $V_M$  values are then normalized to 1  $\mu\text{M}$  of enzyme. Aliquots were withdrawn during the time course of the reaction, and the reactions quenched with EDTA/formamide. Products were separated using sequencing gel electrophoresis, and quantified using photo-stimulated plates and a FujiImager (Fuji). Product formation was fitted to a curve according to Eq. 2.

The dependence of  $V_i$  on NTP concentration is described by the hyperbolic equation:

$$V_i = V_{\max} \cdot (\text{NTP}) / (K_M + (\text{NTP})) \quad (\text{Eq. 3})$$

where  $V_{\max}$  and  $K_M$  are the maximal velocity and the affinity constant of NTP incorporation by NS5B, respectively.  $V_{\max}$  and  $K_M$  were determined from curve-fitting using Kaleidagraph (Synergy Software).

## **ABBREVIATIONS**

HCV, hepatitis C virus; RdRp, RNA dependent RNA polymerase; RNAP, RNA polymerase; RTP, ribavirin triphosphate; IMPDH, inosine 5'-monophosphate dehydrogenase; GTP, guanosine triphosphate; GMP, guanosine monophosphate; HIV, human immunodeficiency virus; RT, reverse transcriptase; WT, wild type; IC<sub>50</sub>, inhibitory concentration 50 %; HPLC high-performance liquid chromatography.

## **ACKNOWLEDGEMENTS**

This work was support by Association Nationale de Recherche sur le Sida (ANRS), by the European Community (Flavitherapeutics European Contract N° QLK3-CT-2001-00506) and by the Centre National de Recherche Scientifique (CNRS).

We thank D. Shlaes, D. Storer, Z. Hong, and L. Tomei for critical reading and improvement of the manuscript. We are grateful to Barbara Selisko and Karine Alvarez for continuous helpful discussions and suggestions.

## REFERENCES

1. Wasley, A., and Alter, M. J. (2000) *Semin Liver Dis* **20**, 1-16
2. Liang, T. J., Rehermann, B., Seeff, L. B., and Hoofnagle, J. H. (2000) *Ann Intern Med* **132**, 296-305
3. Poynard, T., Marcellin, P., Lee, S. S., Niederau, C., Minuk, G. S., Ideo, G., Bain, V., Heathcote, J., Zeuzem, S., Trepo, C., and Albrecht, J. (1998) *Lancet* **352**, 1426-1432
4. McHutchison, J. G., Gordon, S. C., Schiff, E. R., Shiffman, M. L., Lee, W. M., Rustgi, V. K., Goodman, Z. D., Ling, M. H., Cort, S., and Albrecht, J. K. (1998) *N Engl J Med* **339**, 1485-1492
5. Somsouk, M., Lauer, G. M., Casson, D., Terella, A., Day, C. L., Walker, B. D., and Chung, R. T. (2003) *Gastroenterology* **124**, 1946-1949
6. Lauer, G. M., and Walker, B. D. (2001) *N Engl J Med* **345**, 41-52
7. Miller, J., Kigwana, L., Streeter, D., Robins, R., Simon, L., and Roboz, J. (1977) *Ann NY Acad Sci.* **Mar 4**, 211-229.
8. Streeter, D. G., Witkowski, J. T., Khare, G. P., Sidwell, R. W., Bauer, R. J., Robins, R. K., and Simon, L. N. (1973) *Proc Natl Acad Sci U S A* **70**, 1174-1178
9. Vo, N. V., Young, K. C., and Lai, M. M. (2003) *Biochemistry* **42**, 10462-10471
10. Maag, D., Castro, C., Hong, Z., and Cameron, C. E. (2001) *J Biol Chem* **276**, 46094-46098.
11. Gallois-Montbrun, S., Chen, Y., Dutartre, H., Sophys, M., Morera, S., Guerreiro, C., Schneider, B., Mulard, L., Janin, J., Veron, M., Deville-Bonne, D., and Canard, B. (2003) *Mol Pharmacol* **63**, 538-546
12. Schinazi R F, L. B. A., Mellors J W. (2000) *Int. Antiviral News* **8**, 65-91

13. Migliaccio, G., Tomassini, J. E., Carroll, S. S., Tomei, L., Altamura, S., Bhat, B., Bartholomew, L., Bosserman, M. R., Ceccacci, A., Colwell, L. F., Cortese, R., De Francesco, R., Eldrup, A. B., Getty, K. L., Hou, X. S., LaFemina, R. L., Ludmerer, S. W., MacCoss, M., McMasters, D. R., Stahlhut, M. W., Olsen, D. B., Hazuda, D. J., and Flores, O. A. (2003) *J Biol Chem* **278**, 49164-49170
14. Carroll, S. S., Tomassini, J. E., Bosserman, M., Getty, K., Stahlhut, M. W., Eldrup, A. B., Bhat, B., Hall, D., Simcoe, A. L., LaFemina, R., Rutkowski, C. A., Wolanski, B., Yang, Z., Migliaccio, G., De Francesco, R., Kuo, L. C., MacCoss, M., and Olsen, D. B. (2003) *J Biol Chem* **278**, 11979-11984
15. Shim, J., Larson, G., Lai, V., Naim, S., and Wu, J. Z. (2003) *Antiviral Res* **58**, 243-251
16. Menendez-Arias, L. (2002) *Trends Pharmacol Sci* **23**, 381-388
17. Deval, J., Courcambeck, J., Selmi, B., Boretto, J., and Canard, B. (2004) *Curr Drug Metab* **5**, 305-316
18. Oh, J. W., Ito, T., and Lai, M. M. (1999) *J Virol* **73**, 7694-7702
19. Luo, G., Hamatake, R. K., Mathis, D. M., Racela, J., Rigat, K. L., Lemm, J., and Colonno, R. J. (2000) *J Virol* **74**, 851-863.
20. Zhong, W., Uss, A. S., Ferrari, E., Lau, J. Y., and Hong, Z. (2000) *J Virol* **74**, 2017-2022.
21. Choi, K. H., Groarke, J. M., Young, D. C., Kuhn, R. J., Smith, J. L., Pevear, D. C., and Rossmann, M. G. (2004) *Proc Natl Acad Sci U S A* **101**, 4425-4430
22. Butcher, S. J., Grimes, J. M., Makeyev, E. V., Bamford, D. H., and Stuart, D. I. (2001) *Nature* **410**, 235-240
23. Bressanelli, S., Tomei, L., Rey, F. A., and De Francesco, R. (2002) *J Virol* **76**, 3482-3492.

24. Hong, Z., Cameron, C. E., Walker, M. P., Castro, C., Yao, N., Lau, J. Y., and Zhong, W. (2001) *Virology* **285**, 6-11.
25. Lesburg, C. A., Cable, M. B., Ferrari, E., Hong, Z., Mannarino, A. F., and Weber, P. C. (1999) *Nat Struct Biol* **6**, 937-943.
26. Zhong, W., Ferrari, E., Lesburg, C. A., Maag, D., Ghosh, S. K., Cameron, C. E., Lau, J. Y., and Hong, Z. (2000) *J Virol* **74**, 9134-9143.
27. Ranjith-Kumar, C. T., Gutshall, L., Sarisky, R. T., and Kao, C. C. (2003) *J Mol Biol* **330**, 675-685
28. Tomei, L., Altamura, S., Bartholomew, L., Biroccio, A., Ceccacci, A., Pacini, L., Narjes, F., Gennari, N., Bisbocci, M., Incitti, I., Orsatti, L., Harper, S., Stansfield, I., Rowley, M., De Francesco, R., and Migliaccio, G. (2003) *J Virol* **77**, 13225-13231
29. Ranjith-Kumar, C. T., Kim, Y. C., Gutshall, L., Silverman, C., Khandekar, S., Sarisky, R. T., and Kao, C. C. (2002) *J Virol* **76**, 12513-12525
30. Lohmann, V., Roos, A., Korner, F., Koch, J. O., and Bartenschlager, R. (1998) *Virology* **249**, 108-118
31. Lohmann, V., Roos, A., Korner, F., Koch, J. O., and Bartenschlager, R. (2000) *J Viral Hepat* **7**, 167-174
32. Shim, J. H., Larson, G., Wu, J. Z., and Hong, Z. (2002) *J Virol* **76**, 7030-7039
33. Walker, M. P., Appleby, T. C., Zhong, W., Lau, J. Y., and Hong, Z. (2003) *Antivir Chem Chemother* **14**, 1-21
34. Wu, J. Z., and Hong, Z. (2003) *Curr Drug Targets Infect Disord* **3**, 207-219
35. Huang, H., Chopra, R., Verdine, G. L., and Harrison, S. C. (1998) *Science* **282**, 1669-1675.
36. Kao, C. C., Yang, X., Kline, A., Wang, Q. M., Barket, D., and Heinz, B. A. (2000) *J Virol* **74**, 11121-11128.

37. Kao, C. C., Singh, P., and Ecker, D. J. (2001) *Virology* **287**, 251-260.
38. Ranjith-Kumar, C. T., Gutshall, L., Kim, M. J., Sarisky, R. T., and Kao, C. C. (2002) *J Virol* **76**, 12526-12536
39. Vo, N. V., Tuler, J. R., and Lai, M. M. (2004) *Biochemistry* **43**, 10579-10591
40. Lohmann, V., Overton, H., and Bartenschlager, R. (1999) *J Biol Chem* **274**, 10807-10815
41. Adachi, T., Ago, H., Habuka, N., Okuda, K., Komatsu, M., Ikeda, S., and Yatsunami, K. (2002) *Biochim Biophys Acta* **1601**, 38-48
42. Leveque, V. J., Johnson, R. B., Parsons, S., Ren, J., Xie, C., Zhang, F., and Wang, Q. M. (2003) *J Virol* **77**, 9020-9028

## LEGENDS TO FIGURES

**Fig. 1. 2'-O-methyl GTP decreases the incorporation of  $\alpha$ - $^{32}\text{P}$ -GTP by wild-type NS5B into a polyC template.** *A*, Time course of incorporation of [ $^3\text{H}$ ]-GTP (100  $\mu\text{M}$ ) into polyC RNA template (0.1  $\mu\text{M}$ ) in the presence of increasing concentration of 2'-O-methyl GTP analyzed by counting radiolabeled RNA spotted onto DE-81 paper disc as described under "Experimental Procedures". RNA synthesis is represented as GMP incorporation into insoluble product (cpm) as a function of time in presence of none (control,  $\text{O}$ ), 1  $\mu\text{M}$  ( $\square$ ), 50  $\mu\text{M}$  ( $\times$ ) or 500  $\mu\text{M}$  2'-O-methyl GTP ( $\Delta$ ). *B*, [ $^3\text{H}$ ]-GTP (100  $\mu\text{M}$ ) polymerization is measured during 3 min in presence of increasing concentration of 2'-O-methyl GTP. The percentage of polymerase activity is shown as a function of 2'-O-methyl GTP concentration. Fitting of the data to Eq. 1 was used to determine the  $\text{IC}_{50}$  value. *C*, The initial velocity of polymerization of 10 to 500  $\mu\text{M}$  of [ $^3\text{H}$ ]-GTP was measured in the absence of 2'-O-methyl GTP ( $\text{O}$ ), or in the presence of 5  $\mu\text{M}$  ( $\square$ ) or 10  $\mu\text{M}$  2'-O-methyl GTP ( $\diamond$ ). Results are represented under a reciprocal Lineweaver-Burke plot, and data were fitted to a linear equation.  $V_i$  is expressed in  $\text{pmoles product}\cdot\text{sec}^{-1}\cdot\text{pmole}^{-1}\text{enzyme}$ , i.e., in  $\text{sec}^{-1}$ .

**Fig. 2. Ribbon Representation of the  $\Delta 55$ -NS5B polymerase.** Adapted from Bressanelli *et al.* ((23), PDB code 1GX5). Relevant sub-domains, indicated by arrows, are the nucleotide binding site at the active site (N2), the nucleotide binding site at the initiation site (N1), the  $\beta$ -loop (or  $\beta$ -hairpin, flap), and the low affinity surface GTP-binding site encompassing the P495 residue. N and C stand for N-terminus and C-terminus, respectively. The six histidine tag is not represented at the C-terminus.

**Fig. 3. Kinetics of RNA synthesis using NS5B and an oligoC RNA template.** *A*, Wild-type NS5B and oligoC RNA template (10  $\mu$ M) were mixed with  $\alpha$ -<sup>32</sup>P-GTP (10  $\mu$ M, 1 $\mu$ Ci) to start the reaction as described under "Experimental Procedures". At various times (0, 10 s, 30 s, 45 s, 1 min, 5 min, 15 min, 30 min, and 1 h), reaction aliquots were quenched by the addition of EDTA/formamide, and the RNA products were resolved on 20 % polyacrylamide/7M urea gel. M. RNA marker synthesized using T7 RNAP and an appropriate template; each band product is indicated on the right. *B*, The experiment shown in *A* was quantitated and the result is represented as the amount of RNA synthesized ( $\mu$ M) as a function of time for abortive RNA products (2-mer to 6-mer) ( $\diamond$ ), run off product (pppG<sub>15</sub> mers) (O) and total RNA product ( $\square$ ). *C*, The experiment shown in *A* was quantitated and is represented here as the amount of RNA synthesized ( $\mu$ M) as a function of time for pppG<sub>2</sub> products (X), pppG<sub>3</sub> ( $\diamond$ ), pppG<sub>4</sub> ( $\diamond$ ) pppG<sub>5</sub> ( $\square$ ), pppG<sub>6</sub> (O), and pppG<sub>15</sub> ( $\Delta$ ) products.

**Fig. 4. Incorporation of GTP and 2'-O-methyl GTP into RNA during initiation.** *A*, Time course of GTP or 2'-O-methyl GTP incorporation into RNA during initiation was analyzed using 20 % acrylamide denaturing gel electrophoresis as described under "Experimental Procedures". RNA H (-) was used as template for the synthesis of the first phosphodiester bond between GTP or 2'-O-methyl GTP and CTP (100  $\mu$ M, 1  $\mu$ Ci). The pppCC product is the result of internal initiation ((32), see text). 2'-O-methyl GTP incorporation was performed with a 2-fold excess of enzyme to measure accurately low incorporation rates. Migration positions of pppGCC, pppGC and pppCC products are shown with an arrow on the left. *B*, The experiment shown in *A* was repeated for various GTP or 2'-O-methyl GTP concentrations, the pppGpC product was quantitated, and the maximal velocity calculated for each GTP or 2'-O-methyl GTP concentration. Results are represented as the initial velocity for each GTP (O) or 2'-O-methyl GTP ( $\square$ ) concentrations as a function of NTP concentration. 2'-

O-methyl GTP incorporation was performed with a 2-fold excess of enzyme to measure accurately low incorporation rates. Hyperbolic fitting of the data to Eq. 3 was used to determine values of enzymatic constants  $V_{max}$  and  $K_M$ .  $V_i$  is expressed in  $\mu\text{moles product}\cdot\text{sec}^{-1}\cdot\mu\text{mole}^{-1}$  enzyme, i.e., in  $\text{sec}^{-1}$ .

**Fig. 5. The discrimination of 2'-O-methyl GTP during initiation.** *A*, Incorporation of radiolabeled GMP into oligoC RNA template (10  $\mu\text{M}$ ) by NS5B was measured for 30 min in the presence of increasing concentration of 2'-O-methyl GTP (0, 10, 50, 100, 200, 400  $\mu\text{M}$ ), and products were separated using a 20 % acrylamide denaturing gel electrophoresis as described under "Experimental Procedures". Positions of the RNA markers synthesized by T7 RNAP are shown on the left. Accumulation of GMP is shown with an arrow on the right. *B*, The experiment shown in *A* was quantitated and is represented as the amount of RNA synthesized ( $\mu\text{M}$ ) as a function of time for products of 4-mer or less ( $\Delta$ ), pppG5 (X), pppG7 ( $\diamond$ ), and RNA run-off products ( $\geq\text{G15}$ ) ( $\square$ ).

**Fig. 6. Incorporation of GTP and 2'-O-methyl GTP during elongation by WT and  $\Delta$ -flap NS5B.** *A*, Time course incorporation of GTP or 2'-O-methyl GTP during elongation was analyzed by 14 % acrylamide denaturing gel electrophoresis as described under "Experimental Procedures". 5'  $\alpha$ - $^{32}\text{P}$  end-labeled RNA hairpin template (1 $\mu\text{M}$ ) was used to measure the incorporation of GTP or 2'-O-methyl GTP (500  $\mu\text{M}$ ) by wild-type NS5B (1 $\mu\text{M}$ ). 2'-O-methyl GTP incorporation was performed using a 2-fold excess of enzyme to measure low incorporation rates accurately. Migration positions of hairpin and hairpin +1 template are shown with an arrow on the left. The experiment shown in *A* was repeated for various GTP or 2'-O-methyl GTP concentrations, +1 product was quantitated, and the maximal velocity calculated for each GTP or 2'-O-methyl GTP concentration. Results are represented as the

initial velocity for each GTP (○) or 2'-O-methyl GTP (□) concentrations as a function of NTP concentration. Hyperbolic fitting of the data to Eq. 3 was used to determine values of enzymatic constants  $V_{\max}$  and  $K_M$ .  $V_{\max}$  is expressed in pmoles product. $\text{sec}^{-1}$ . $\text{pmole}^{-1}$  enzyme, i.e., in  $\text{sec}^{-1}$ . *B*, Same experiment as described in *A* except that the NS5B  $\Delta$ -flap enzyme was used instead of wild-type NS5B and that reactions with 2'-O-methyl GTP were conducted with 1  $\mu\text{M}$  of enzyme instead of 2 (see "Experimental Procedures").  $V_{\max}$  is expressed in pmoles product. $\text{sec}^{-1}$ . $\text{pmole}^{-1}$  enzyme, i.e., in  $\text{sec}^{-1}$ .

**Fig. 7. Incorporation of GTP by P495L NS5B during elongation.** *A*, Time course GMP incorporation into RNA using an oligoC RNA as a template and wild-type or P495L NS5B. Reactions were performed as described under "Experimental Procedures" using  $\alpha$ - $^{32}\text{P}$ -GTP (100  $\mu\text{M}$ , 1  $\mu\text{Ci}$ ) together with 400 nM and 1 $\mu\text{M}$  of wild-type and P495L NS5B, respectively. Positions of the RNA markers (M) synthesized using T7 RNA polymerase are shown on the left. *B*, Comparative quantitation of the reaction products from the experiment shown in panel *A*. Each individual  $\text{P}_i$  band product from wild-type and P495L NS5B was quantitated using PhosphorImaging analysis, and the ratio of wild-type( $\text{P}_i$ )/P495L( $\text{P}_i$ ) products plotted for each *i*-mer product relative the standard wild-type( $\text{P}_2$ )/P495L( $\text{P}_2$ ) taken as unity.

Table I

*Steady state constants of wild-type,  $\Delta$ -flap, and P495L NS5B polymerase for RNA templates during initiation. Discrimination is determined as the ratio  $(V_{max}/K_M)_{GTP}/(V_{max}/K_M)_{2'-O-methyl\ GTP}$ .*

<i>Nucleotides</i>	WT		$\Delta$ -flap		P495L	
	<i>GTP</i>	<i>2'-O-meGTP</i>	<i>GTP</i>	<i>2'-O-meGTP</i>	<i>GTP</i>	<i>2'-O-meGTP</i>
$K_M$ ( $\mu$ M) <sup>a</sup>	8.5 $\pm$ 0.8	205 $\pm$ 25	15 $\pm$ 1.7	70 $\pm$ 3	7.6 $\pm$ 0.6	130 $\pm$ 25
$V_{max}$ (sec <sup>-1</sup> ) <sup>a</sup>	9.2 $\pm$ 0.2 $10^{-3}$	1.4 $\pm$ 0.06 $10^{-3}$	3.7 $\pm$ 0.09 $10^{-3}$	1.1 $\pm$ 0.01 $10^{-3}$	15.9 $\pm$ 0.3 $10^{-3}$	1.6 $\pm$ 0.1 $10^{-3}$
$V_{max}/K_M$ (sec <sup>-1</sup> / $\mu$ M)	1 $10^{-3}$	6.7 $10^{-6}$	2.7 $10^{-4}$	1.6 $10^{-5}$	2 $10^{-3}$	1.3 $10^{-5}$
Discrimination	148-fold		17-fold		157-fold	

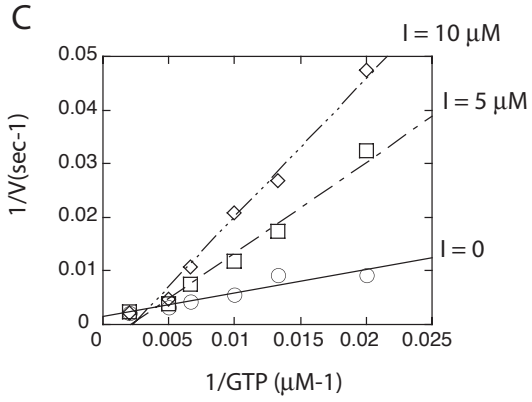
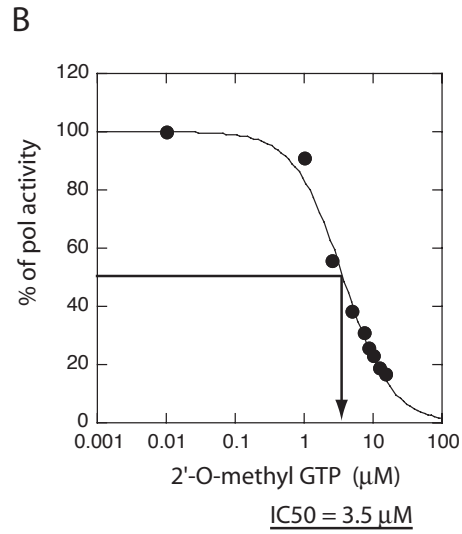
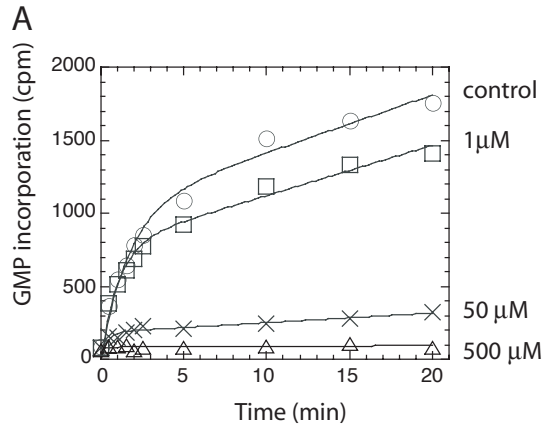
<sup>a</sup>  $K_M$  and  $V_{max}$  were calculated as described under « Experimental Procedures».  $V_{max}$  is expressed in pmoles.sec<sup>-1</sup>.pmole<sup>-1</sup> enzyme.

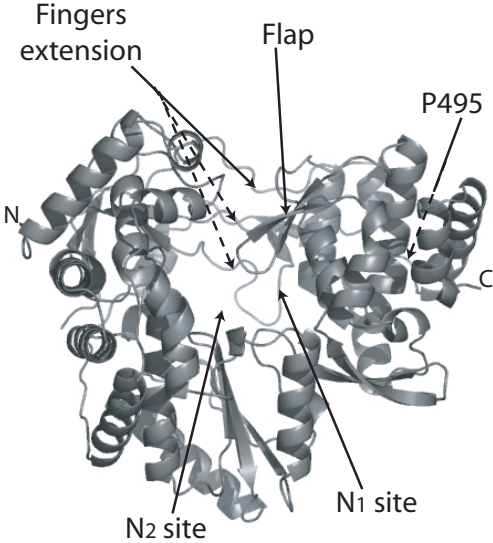
Table II

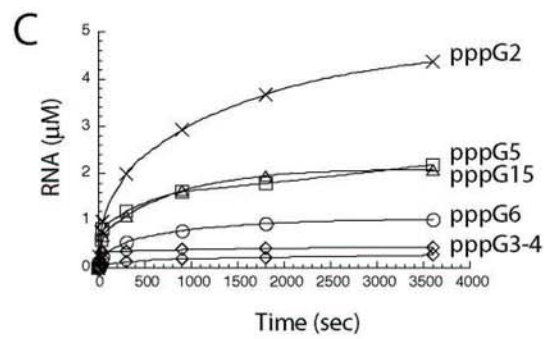
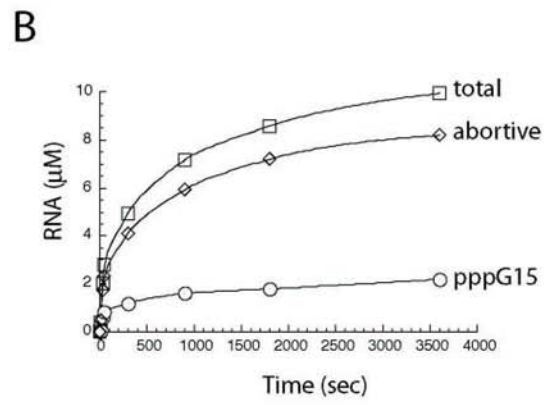
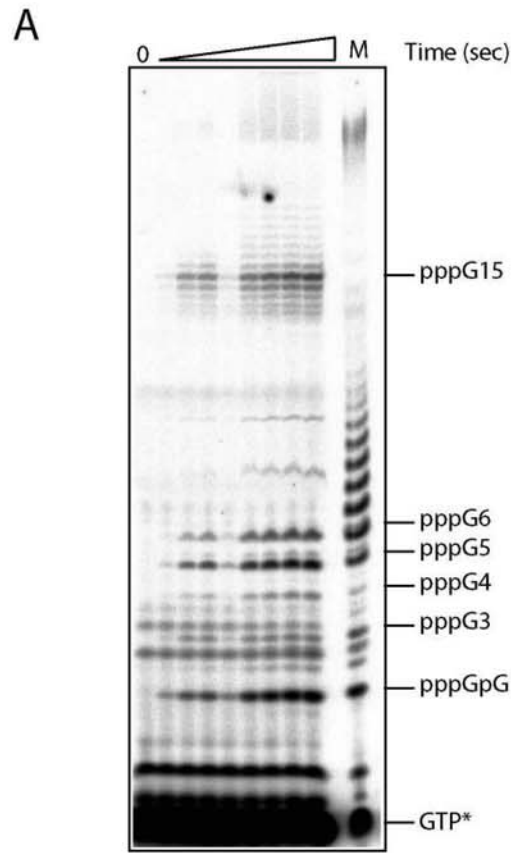
*Steady state constants of wild-type, and  $\Delta$ -flap NS5B polymerase on RNA templates during elongation. Discrimination is determined as the ratio  $(V_{max}/K_M)_{GTP}/(V_{max}/K_M)_{2'-O-methyl\ GTP}$ .*

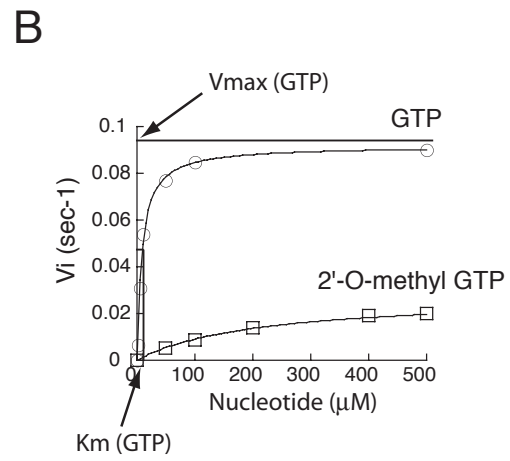
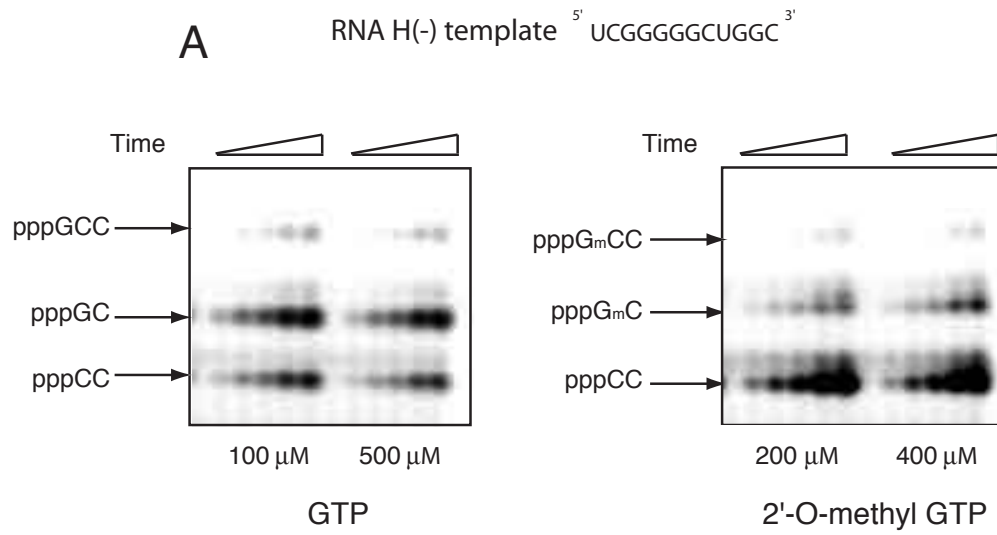
<i>Nucleotides</i>	WT		$\Delta$ -flap	
	<i>GTP</i>	<i>2'-O-meGTP</i>	<i>GTP</i>	<i>2'-O-meGTP</i>
$K_M$ ( $\mu$ M)	47 $\pm$ 14	36 $\pm$ 17	3.3 $\pm$ 0.9	18.3 $\pm$ 2.5
$V_{max}$ ( $\text{sec}^{-1}$ ) <sup>a</sup>	5 $\pm$ 0.5 $10^{-3}$	1.5 $\pm$ 0.5 $10^{-3}$	0.2 $\pm$ 0.005	0.2 $\pm$ 0.005
$V_{max}/K_M$ ( $\text{sec}^{-1}/\mu\text{M}$ )	0.1 $10^{-3}$	0.04 $10^{-3}$	0.055	0.01
Discrimination	2.3-fold		5.5-fold	

<sup>a</sup>  $V_{max}$  is expressed in % of GTP incorporated in hairpin template/sec, normalized per  $\mu$ M enzyme as described under « Experimental Procedures ».

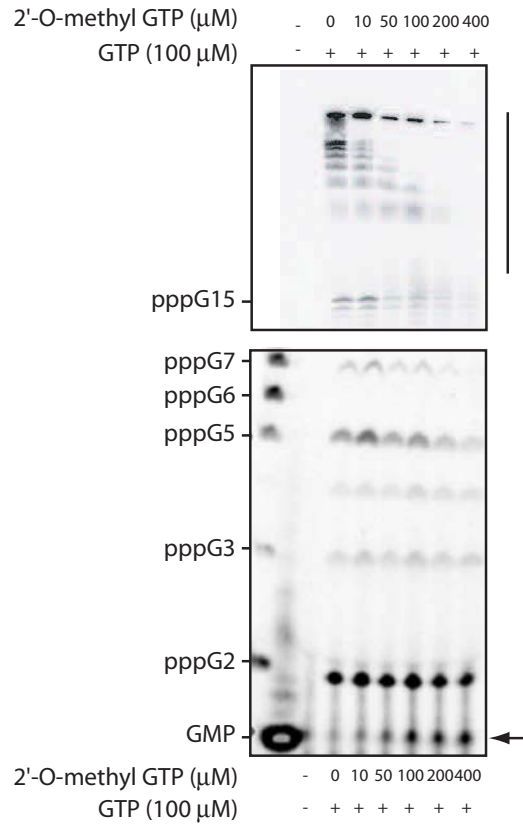




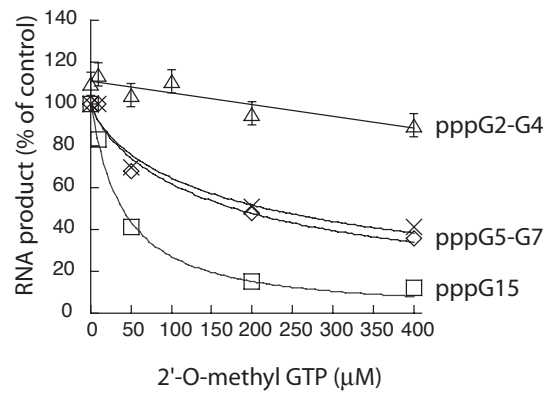


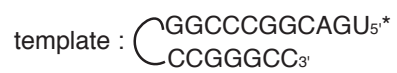


**A**

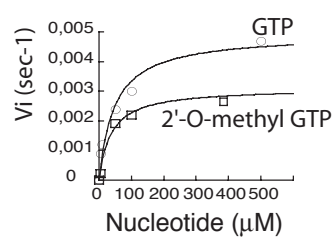
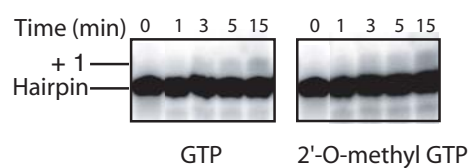


**B**

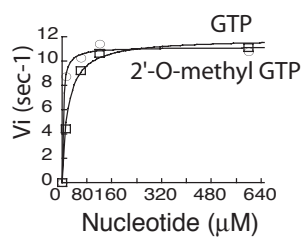
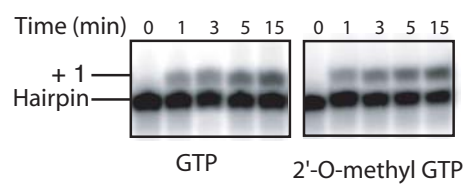


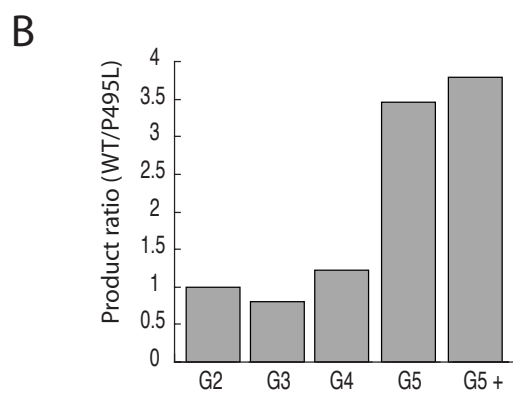
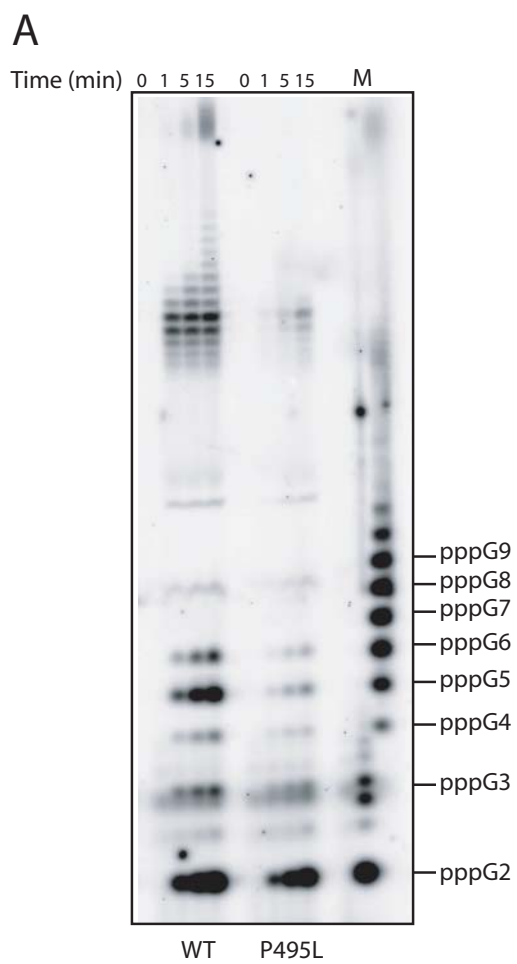


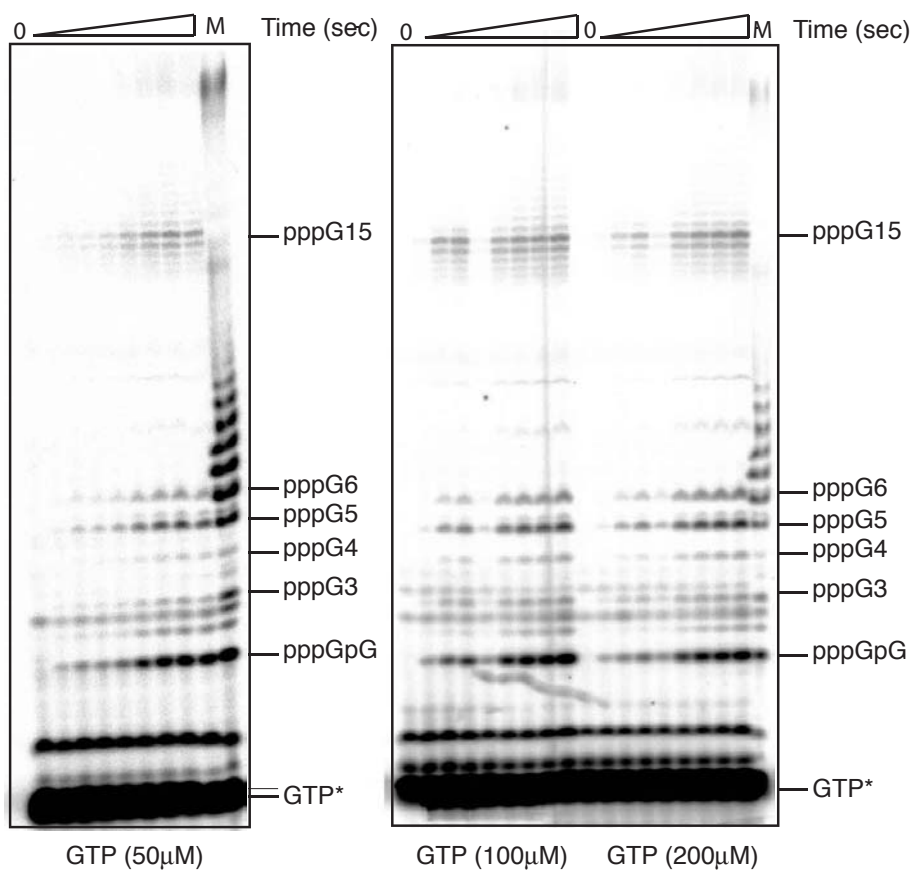
A



B







**Kinetics of RNA synthesis using NS5B and an oligoC RNA template.** Wild type NS5B and oligoC RNA template (10μM) were mixed with  $\alpha$ -<sup>32</sup>P-GTP (1μCi) at the concentration indicated in the figure. At various times (0, 10 s, 30 s, 45 s, 1 min, 5 min, 15 min, 30 min, and 1 h) reaction aliquots were quenched by the addition of EDTA/formamide, and the RNA products were resolved on 20% polyacrylamide/7M urea gel. M. RNA marker synthesized using T7 RNAP and an appropriate template; each band product is indicated on the right.